Selective Small-Diameter Metallic Single-Walled Carbon Nanotube Removal by Mere Standing with Anthraquinone and Application to a Field-Effect Transistor

ARTICLE *in* THE JOURNAL OF PHYSICAL CHEMISTRY C · NOVEMBER 2010

Impact Factor: 4.77 · DOI: 10.1021/jp106398k

Selective Small-Diameter Metallic Single-Walled Carbon Nanotube Removal by Mere Standing with Anthraquinone and Application to a Field-Effect Transistor

Zhi Dai,[†] Liangyu Yan,[†] Sk. Mahasin Alam,[†] Junluo Feng,[†] Pyria Rose Divina Mariathomas,[†] Yuan Chen,[†] Chang Ming Li,[†] Qing Zhang,[‡] Lain-Jong Li,[§] Kok Hwa Lim,*[,†] and Mary B. Chan-Park*[,†]

School of Chemical and Biomedical Engineering, School of Electrical and Electronic Engineering, and School of Materials Science and Engineering, Nanyang Technological University, 62 Nanyang Drive, Singapore 637459, Singapore

Received: July 11, 2010; Revised Manuscript Received: October 27, 2010

Small-diameter metallic single-wall carbon nanotubes (SWNT) were separated from larger diameter semiconducting SWNT when CoMoCAT samples (supplied with abundance of (6,5) species) were left standing at ambient laboratory condition for a few days in dimethylformamide solution containing ethylanthraquinone (EAQ). SWNT enriched in larger diameter semiconducting species by this method were used to fabricate SWNT network-based thin film transistors (TFTs). The resulting devices had mobilities of 0.2 $cm^2/(V\ s)$ and on/off ratios of about 10^4. The on/off ratios were greatly improved, by approximately 2 orders of magnitude, over those of TFTs made with pristine SWNT. The enrichment in semiconducting tubes was corroborated by UV−vis−NIR absorption, photoluminescence excitation (PLE), and resonance Raman scattering spectroscopy. Density functional simulations show that hydroxyl radicals preferentially attack small-diameter metallic and then small-diameter semiconducting nanotubes over larger diameter semiconducting tubes. We propose that EAQ forms radicals in ambient lighted conditions, resulting in this diameter- and metallicity-selective reaction which increases the density of the target species, promoting their sedimentation under centrifugation. This simple method of obtaining semiconducting-enriched SWNT samples should be widely applicable for printed electronic devices.

1. Introduction

Single-walled carbon nanotubes (SWNT) have been shown to have superior field-effect behavior, which makes them an attractive material for use in field-effect transistors (FETs).[1−3] However, as-synthesized SWNT samples usually contain mixtures of metallic (about 1/3 of the SWNT species present) and semiconducting (about 2/3 of the species) nanotube species. The presence of too many metallic tubes impairs or destroys the switching behavior of the FET active channel, and so these must be removed or destroyed for high performance FETs.[4,5] Further, to minimize the impact of tube-to-tube variation, the use of networks of many SWNT, rather than individual nanotubes, has recently been proposed as the active component of FETs.[4−9] The averaging effect in SWNT networks reduces device variability but also places greater demands on removal of metallic nanotubes. Numerous approaches have been taken to separate semiconducting from metallic SWNT.[10−27] FETs employing sorted SWNT networks (SWNTnets) in the active channel have been shown to have high performance and also to be relatively reproducible, as well as printable, offering a route toward low-cost printed macroelectronics.[4−9] However, many of the proposed separation methods may not easily achieve full semiconductor device yield or may involve substantial costs.

Separation strategies include the synthetic strategy of selective growth, postsynthesis solution-based separation methods (such as electrophoretic separation, dielectrophoresis,[10−12] chromatography,[13] density gradient ultracentrifugation (DGU),[14−16] gel-based separation techniques,[17] selective aromatic extraction,[18−20] surfactant extraction,[21−23] amine extraction,[13] surface alignment,[13] and selective polymer wrapping[24] and fabrication-based techniques such as electrical breakdown of metallic nanotubes.[6,25] Selective functionalizations of SWNT using small aromatic molecules, which can strongly interact with SWNT via $\pi-\pi$ stacking interaction, have been used for selective separation of SWNT.[18−20] Such molecules include diazonium salts,[26] pyrene derivatives, porphyrin derivatives, pentacene derivatives, and flavin mononucleotide.[18,27] However, most separation techniques do not yet produce SWNT samples of sufficient semiconducting purity to meet the requirements for electronic devices or are expensive.

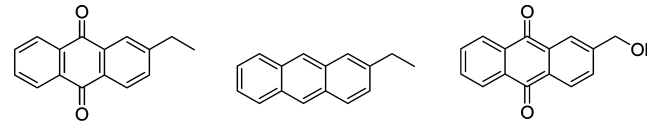

(a) (b) (c)

Figure 1. Structures of (a) 2-ethylanthraquinone (EAQ), (b) EAC, and (c) HMAQ.

In this work, we describe a simple method for the selective removal of metallic SWNT using the small aromatic molecule 2-ethylanthraquinone (EAQ) (Figure 1a), which preferentially attacks smaller diameter, particularly metallic, species of CoMoCAT SWNT dispersed in dimethylformamide (DMF). The CoMoCAT sample (SWeNTSG65 with at least 90 wt % carbon

* Corresponding authors. E-mail: KokHwa@ntu.edu.sg (K.H.L.); mbechan@ntu.edu.sg (M.B.C.-P.). Tel: (65) 6790 6064. Fax: (65) 6792 4062.
[†] School of Chemical and Biomedical Engineering.
[‡] School of Electrical and Electronic Engineering.
[§] School of Materials Science and Engineering.

10.1021/jp106398k
Published on Web 11/19/2010

purity) have species distributions weighted toward the (6, 5) semiconducting species. The pristine SWNT were suspended in DMF solution containing EAQ and left standing for a few days. After standing, the SWNT/DMF/EAQ solutions were centrifuged to remove nanotube bundles and individual nanotubes attacked by EAQ. Selective attack and precipitation of smaller diameter metallic species would result in enrichment of the remaining suspended population of tubes in larger diameter semiconducting species. The supernatant SWNT solution was filtered, and the SWNT were washed and then resuspended in 1% sodium dodecyl sulfate (SDS) aqueous solution for spectroscopic characterizations and FET fabrication. Ultraviolet visible near-infrared (UV−vis−NIR) spectroscopy, photoluminescence excitation (PLE) spectroscopy, resonant Raman scattering (RRS) spectroscopy, and electrical performance of fabricated FET devices were used to evaluate the quality of the separation. The selectivity of EAQ for smaller diameter metallic nanotubes was verified using density functional calculations. The selection effects of other anthraquinones (specifically 2-(hydroxymethyl)anthraquinone (HMAQ) and anthracene (EAC) (Figure 1b,c) were also studied experimentally.

2. Experimental Section

SWNT produced by the CoMoCAT process (SWeNTSG65 with at least 90 wt % carbon purity) were purchased from Southwest Nanotechnologies. The as-supplied CoMoCAT SWNT have a narrow chiral species distribution dominated by the (6,5) species. Dimethylformamide (DMF) was used for the SWNT dispersion.[28] 2-Ethylanthraquinone and other chemicals were purchased from Sigma-Aldrich, unless otherwise specified. The preparation of semiconducting-SWNT-enriched solutions was as follows. A mixture of SWNT powder (1 mg), EAQ (50 mg), and DMF (30 mL) was homogenized by sonication for 10 min using a water-bath sonicator and for 20 min using a tip ultrasonicator at 80 W in an ice bath. The SWNT finely dispersed in EAQ/DMF solution were left standing in ambient conditions for 7 days. Then the suspension was centrifuged for 1 h at 10 000 g to remove the metallic SWNT, nanotube bundles, and other impurities. Subsequently, the homogeneous supernatants were collected and filtered through a polytetrafluoroethane (PTFE) membrane (0.2 μm). The SWNT solids were washed with DMF (50 mL) and dichloromethane (50 mL). The SWNT were then redispersed in DMF (50 mL) and filtered through a PTFE membrane (0.2 μm), redispersed in acetone (50 mL), filtered through a PTFE membrane (0.2 μm), and finally redispersed in ethanol (50 mL), filtered through a PTFE membrane (0.2 μm), and dried overnight at 120 °C to yield semiconductor-enriched SWNT solids. These were redispersed in 20 mL of 1% sodium dodecyl sulfate (SDS) DI water solution by sonication for 10 min using a tip ultrasonicator set at 80 W in an ice bath for spectroscopic and electrical properties measurements.

Ultraviolet (UV)−visible (vis)−near-infrared (NIR) absorption spectroscopy was conducted in transmission mode on a Varian Cary 5000 UV−vis−NIR spectrophotometer. Fluorescence characterization was performed on a Jobin-Yvon Nanolog-3 spectrofluorometer with an InGaAs detector. Raman spectra of the samples were measured with a Renishaw Ramanscope in the backscattering configuration, and Stokes spectra of the samples were obtained with 514.5 and 633 nm lasers. Atomic force microscopy (AFM) was conducted using a MFP 3D microscope (Asylum Research, Santa Barbara, CA) with a cantilever (Arrow NC, Nanoworld) in ac mode.

For electrical resistivity measurements, after the separation procedure the homogeneous supernatant was collected and filtered through a polytetrafluoroethane (PTFE) membrane (0.2 μm). The solid SWNT were washed with DMF (50 mL), dichloromethane (50 mL), and ethanol (50 mL) and then were dried overnight at 120 °C to produce a semiconductor-enriched SWNT film. The precipitate was also washed with DMF, dichloromethane, and ethanol and dried overnight at 120 °C to produce a metallic-enriched SWNT film. A resistance meter (Keithley 2400 source meter) with a four-point probe (Signatone Pro4 probe) was used to measure the electrical resistivity of the samples.

For FET fabrication, SWNT were deposited on Au electrodes which permitted the efficient testing of various SWNT samples. The channel length (source-drain distance) was 20 μm and the channel width was 60 μm. The gate dielectric was a 300 nm SiO_2 layer. The FET devices were fabricated by a simple drop-casting method from semiconducting-enriched SWNT solution. Sixty devices were fabricated of each type (60 electrode pairs were created on each substrate). All electrical measurements were carried out in ambient conditions using a Keithley semiconductor parameter analyzer, model 4200-SCS.

For the computer simulations, all the calculations were performed using generalized gradient approximation Perdew−Burke−Eznerhof (GGA-PBE) method[29] as implemented in Vienna ab initio simulation package (VASP).[30] A $1 \times 1 \times 1$ grid for k-point sampling and an energy cutoff of 400 eV were used throughout our calculations. In this study, we used •OH radical as the model radical to understand the interaction between EAQ radical and single-walled carbon nanotubes (SWCNTs). The bindings with various small- and large-diameter semiconducting and metallic SWNT species (Table 3) were investigated.

3. Results and Discussion

Figure 2a and 2b show the photoluminescence excitation (PLE) maps of pristine and EAQ-separated SWNT. PLE spectroscopy detects only semiconducting species. When a specific nanotube chirality species is excited with energy similar to its secondary E_{22} transition, that species emits energy corresponding to its primary E_{11} transition.[31] Table 1 summarizes the relative abundances of various species, taking into account the different PL quantum efficiencies of the species. For the pristine sample, Table 1 and Figure 2a show that the intensity due to the (6,5) species is much stronger than those of (8,3), (7,5), and (8,4) species. Table 1 and Figure 2b also show that after separation with EAQ, the (6,5) species still dominates the PLE map but the intensities of the (7,5), (7,6), and (8,4) species increase, relative to (6,5), compared to before separation. The decrease of relative abundances of (6,5) and (8,3) species indicates that EAQ preferentially attacks smaller diameter semiconducting SWNT and causes them to precipitate under centrifugation. Figure 2c clearly shows that sem-SWNT having larger diameters (i.e., (7,5), (8,4), and (7,6) are enriched relative to sem-SWNT with smaller diameters (i.e., (6,5) and (8,3)) after treatment with EAQ.

It is generally reported that pristine CoMoCAT SWNT have diameters ranging from 0.7 to 0.9 nm so that, according to the Kataura plot, Raman resonance scattering (RRS) excitation with 514.5 nm (2.41 eV) and 633 nm (1.96 eV) probes both metallic and semiconducting nanotubes as shown in Figure 3ia and 3iia.[32,33] The radial breathing mode (RBM) peaks, typically in the 100−400 cm^{-1} range, are inversely proportional to the nanotube diameter. Figure 3ia shows the RRS spectra of pristine and EAQ-separated SWNT under 514 nm excitation: the smaller (7,4) metallic nanotubes are distinctly decreased while the larger

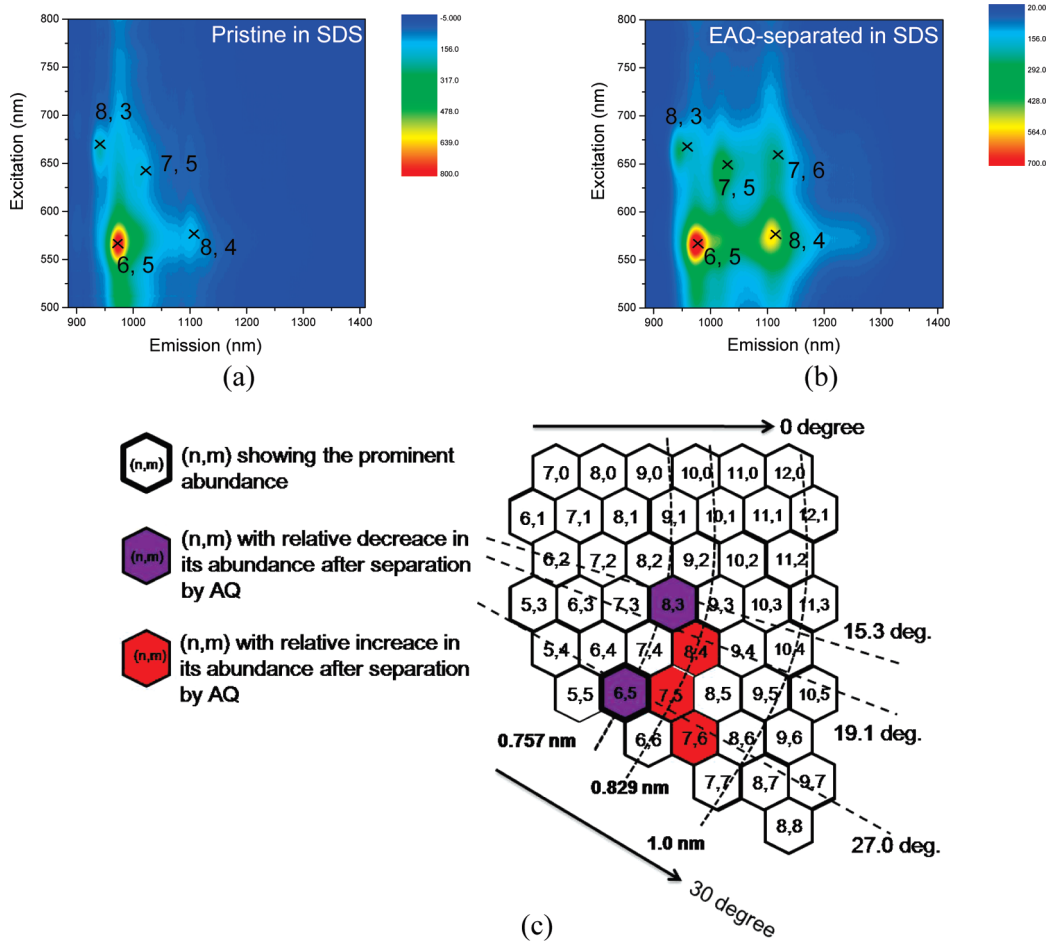

Figure 2. PLE intensity map as a function of excitation and emission wavelength for (a) pristine SWNT and (b) for SWNT after treatment with 2-ethylanthraquinone. (c) Graphene sheet map: summary of enrichment in (*n*,*m*) abundance with extraction of SWNT with 2-ethylanthraquinone.

TABLE 1: CoMoCAT Semiconducting Species Abundance before and after EAQ Separation[a]

				before separation		after separation	
(*n*, *m*)	diameter (nm)	chiral angle (deg)	calculated intensity	relative PL peak intensity, %	calibrated PL intensity, %	relative PL Peak intensity, %	calibrated PL intensity, %
(6,5)	0.757	27.0	0.67	67.5	72.9	45.9	44.1
(8,3)	0.782	15.3	2.13	16.7	5.7	10.7	3.2
(7,5)	0.829	24.5	0.71	6.3	6.4	15.7	14.2
(8,4)	0.840	19.0	0.46	9.5	15.0	22.2	31.0
(7,6)	0.895	27.5	0.47	0	0	5.5	7.5

[a] (6,4) is not detectable by PLE in the wavelength range of our machine.

diameter (8,5) metallic nanotube concentration seems not to be changed by the EAQ treatment. In the RBM spectra obtained using 633 nm laser (Figure 3iia), the peaks at about 262 cm^{-1}, 283 cm^{-1}, 295 cm^{-1}, 310 cm^{-1}, and 333 cm^{-1} are attributed to semiconducting (7,6), (7,5), (8,3), (6,5), and (6,4) species, respectively. Treatment with EAQ diminished the abundance of the smaller diameter semiconducting (6,4) and (6,5) species relative to the larger diameter species ((7,5), (8,3), etc.) (Table 2), corroborating the PL results (Table 1). Further, Figure 3ib and 3iib shows that the G-band at about 1540 cm^{-1} due to metallic nanotube species was reduced after EAQ separation, indicating reduction of metallic tube concentration.[25,26] The PLE and Raman data show that smaller diameter species, whether metallic or semiconducting, are depleted after EAQ treatment.

In addition to diameter selectivity, we investigated the possibility of metallicity preference of EAQ. Figure 4a shows the UV−vis−NIR spectra of pristine and EAQ-separated SWNT. The pristine SWNT show UV−vis−NIR absorption peaks in the 400−490 nm range due to the metallic species first van Hove electronic transitions (M_{11}). After mixing SWNT with EAQ/DMF solution and finally dispersing in 1% SDS solution under the same conditions as for pristine SWNT, M_{11} peaks were found to be selectively suppressed, indicating relative depletion of metallic tubes with respect to semiconducting tubes.

To confirm the metallic versus semiconducting separation effect of EAQ, electrical properties of pristine and separated fractions of SWNT networks were also measured. The electrical resistivities of SWNT networks made from the metallic and semiconducting fractions were, respectively, 191 Ω/cm^2 and 62 216 Ω/cm^2, which are significantly lower and higher than that of pristine SWNT (1020 Ω/cm^2), corroborating the metallicity-based separation.

Field effect transistors (FETs) with SWNT networks as the active channels were also tested. Devices obtained from sem-

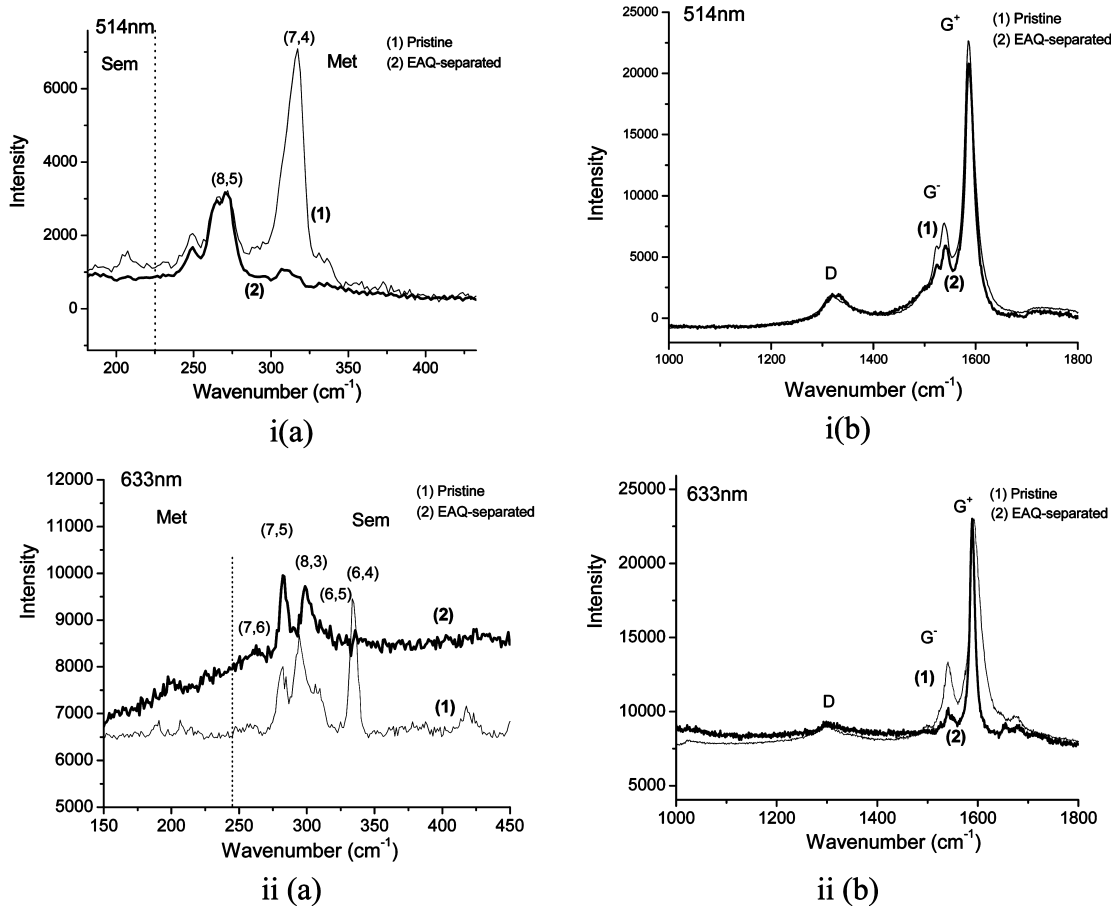

Figure 3. Raman spectra of (1) pristine SWNT and (2) SWNT after treatment with 2-ethylanthraquinone (i) using a 514 nm laser and (ii) using a 633 nm laser. (a) The RBM region. (b) Raman D and G bands.

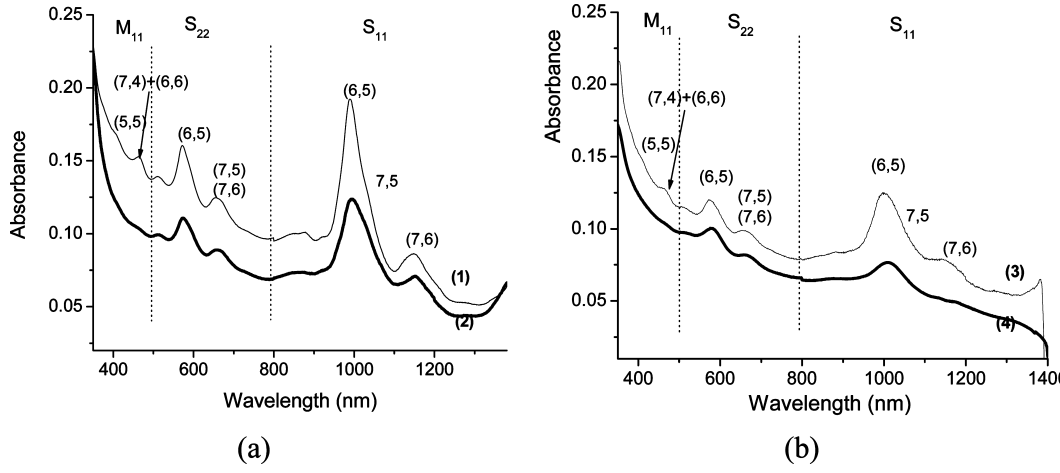

Figure 4. Optical absorption spectra of (1) pristine SWNT, (2) SWNT after treatment with EAQ, (3) SWNT after treatment with EAC, and (4) SWNT after treatment with 2-(hydroxymethyl)anthraquinone.

SWNT-enriched samples with lower metallic nanotube content should exhibit on−off ratios higher than those of devices made with pristine SWNT samples under the same fabrication and characterization conditions. We tested and compared TFTs made with EAQ-separated and pristine SWNT networks. AFM measurement of the SWNT network between the source and drain shows the nanotube film thickness to be about 10 nm. The SWNT network density in the channel area is around 10−20 tubes/μm^2 (Figure 5a). Figure 5b shows the transfer curve of a representative TFT device with forward sweep of drain current (I_d) vs gate voltage (V_g). The FET exhibited p-type behavior with an on/off ratio of 10^4. Mobility was estimated to be 0.2 cm^2/(V s) using the standard formula $\mu = (dI_d/dV_g)/(\varepsilon V_d W/L_{ox}L)$, where L_{ox} is the SiO_2 thickness, L is the channel length, ε is the dielectric constant of SiO_2 (4.0), and W is the channel width. Figure 5c shows a histogram of on/off ratios for devices constructed on the same substrate material with EAQ-separated SWNT and with pristine SWNT. The sample size for each type of SWNT device is 60. The pristine SWNT−TFTs show a broad distribution of on/off ratios from 5 to 1000: 83% of the TFTs had on/off ratios lower than 100 and none of the TFTs had on/off ratios higher than 10^4. By contrast, all the on/off ratios of the EAQ-separated SWNT−TFTs were distributed between 10^3 and 10^5, 75% of the TFTs had on/off ratios higher than 10^4,

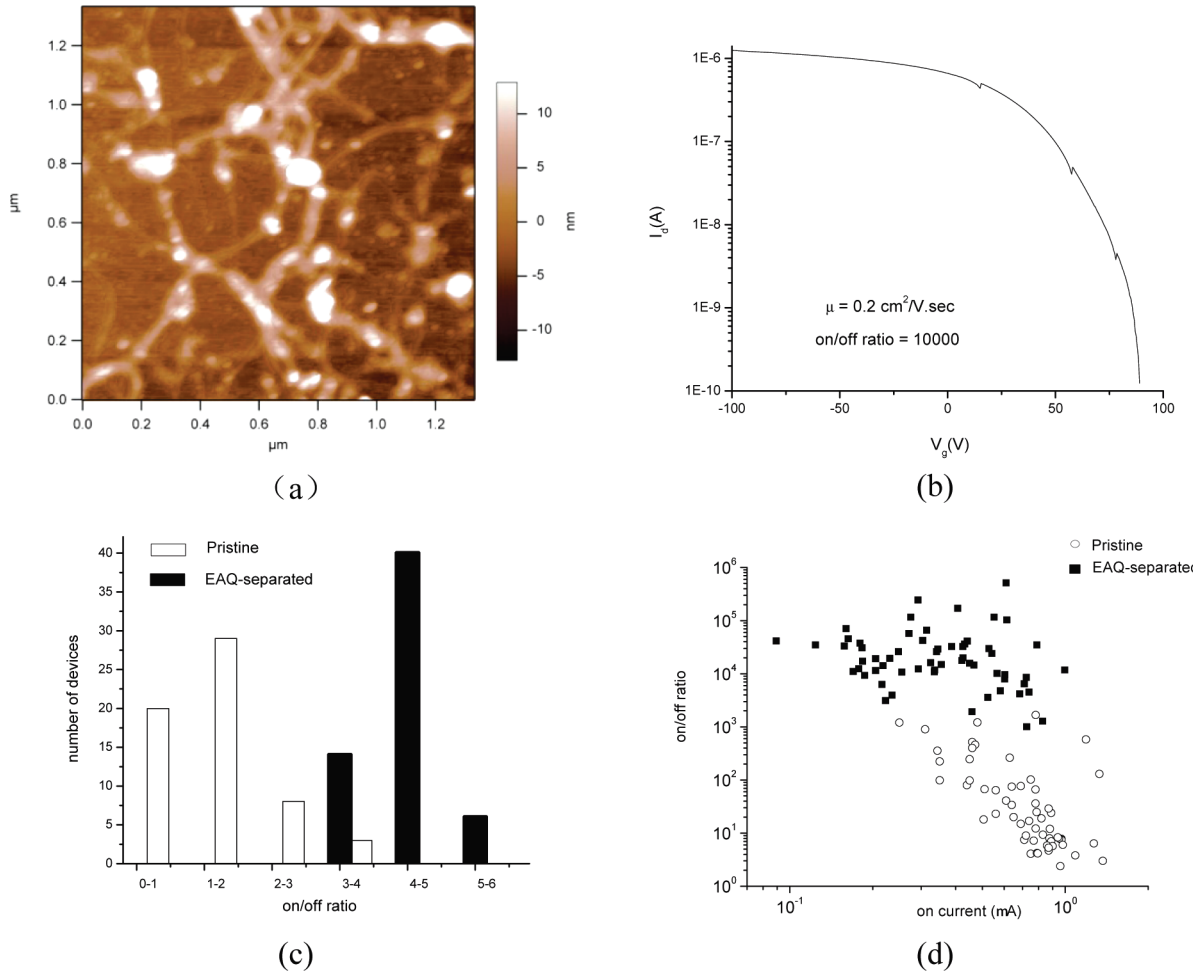

Figure 5. (a) AFM image of SWNT or bundles on SiO_2/Si substrate between source/drain electrodes. (b) Transfer characteristics (V_{DS} = 2 V) for forward sweeps of I_{DS} vs V_{GS} for bottom-gated FETs drop-cast with SWNT solution after treatment with 2-ethylanthraquinone. (c) Histogram of distribution of I_{on}/I_{off} ratios. We characterized sixty devices for pristine SWNT (white) and SWNT after treatment with 2-ethylanthraquinone (black). (d) On-state current (I_{on}) plotted against on/off ratio of 60 devices for pristine SWNT (white) and SWNT after treatment with 2-ethylanthraquinone (black).

and none of the TFTs had an on/off ratio lower than 10^3. Figure 5d shows the on/off ratio versus the on-state current (I_{on}) for the devices made with EAQ-separated SWNT and pristine SWNT; the on/off ratio of the EAQ-separated SWNT−TFTs is significantly improved (by ∼2 orders of magnitude) above that of the pristine SWNT−TFTs. These results clearly demonstrate that EAQ preferentially suspends semiconducting nanotubes and removes the metallic tubes so that better TFTs are made.

We employed density functional calculations to model the interaction of EAQ with various semiconducting and metallic nanotube species present. It has been reported that approximately 40% of a CoMoCAT sample is (6,5) and the semiconducting and metallic species present in CoMoCAT present are approximately in the abundance ratio of 11:1.[32] The most abundant metallic species present is (7,4) which has a fairly small diameter of 0.75 nm,[33] close to that of the dominant (6,5) semiconducting species present. Binding energies of the •OH radical, which was used as a proxy for EAQ radicals, with various semiconducting ((6,4), (6,5), (7,5), and (8,4)) and metallic ((8,2), (7,4), and (10,1)) nanotubes were calculated (Table 3). (The (8,2) and (10,1) species are not found in actual CoMoCAT samples but added to show the effect of diameter on metallic nanotube binding.) We found that the EAQ molecule does not bind to the semiconducting or metallic SWNT so that the binding energy is zero (see Table 3), which is consistent with the report by Woods et al.[34] that benzene is only physisorbed on SWNT (8,0) with an equilibrium distance of ∼3.15 Å above the SWNT. However, it is generally known that EAQ can form radicals under UV,[35] and from our current density functional calculations, we found that •OH radical interacts with all the metallic and semiconducting species with binding energies between −1.77 eV and −1.20 eV, forming a single bond between C and O with a bond distance of ∼1.47 Å (see Table 3 and Figure 6). We interpret the active species responsible for the enrichment of semiconducting SWNT to be radicals from EAQ formed from ambient illumination.

Figure 7 shows that the binding of •OH radical with metallic nanotubes is stronger (i.e., more negative) than with semiconducting tubes of similar diameter. For example, (7,4) binds more strongly by −0.28 eV than (6,5), and these two tubes, which have about the same diameter (∼7.6 Å), are respectively the most abundant metallic and semiconducting species present in this grade of CoMoCAT SWNT. Further, smaller diameter tubes (both semiconducting and metallic) have stronger interaction with the radical than larger diameter nanotubes of the same metallicity. These trends are consistent with our FET measurement that EAQ preferentially suspends semiconducting nanotubes and attacks/removes metallic tubes so that better FETs are observed. Raman and UV−vis−NIR data (Figures 3ia and

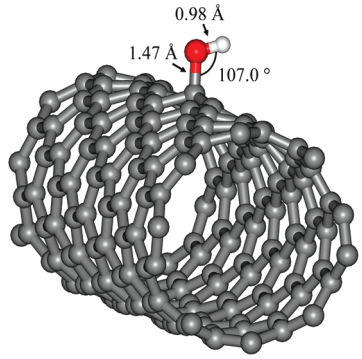

Figure 6. Pertinent geometries of •OH radical adsorption on metallic SWNT (8,2). Gray spheres, C; red sphere, O; white sphere, H.

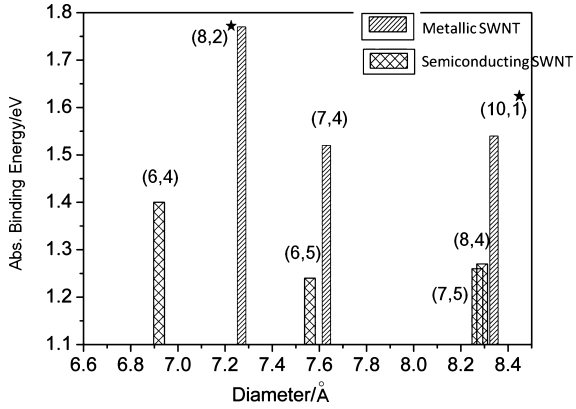

Figure 7. Effect of metallicity and diameter on binding energy with •OH radical (the binding energy is negative but the absolute value is shown) (★: indicates model species for this study of the effect of diameter).

4a) also confirm the removal of (7,4) species which is the most abundant metallic species and has relatively small diameter. However, Figure 3ia also suggests that the larger diameter (8,5) metallic tubes still remain in the SWNT ensemble. Using CoMoCAT SWNT, which have narrow initial chirality range initially, it is clear that treatment with EAQ in DMF preferentially removes smaller diameter metallic nanotubes, resulting in enrichment in larger diameter semiconducting species.

EAQ, which has a very short alkyl chain, has no dispersion effect on SWNT; this is obvious from the very low concentration of SWNT suspended in a poor SWNT-solvating solvent such as toluene. For many other organic moiety-functionalized SWNT, the organic molecule generally has a long chain, such as a long alkane chain, polyethylene glycol, or a polymer, to increase the nanotube dispersibility. The very short alkyl chain of EAQ provides no improvement in the dispersion of SWNT. We propose that SWNT can disperse well in DMF, and during the standing of the SWNT solution in ambient light, some of the EAQ is photoactivated into radicals in small quantities which preferentially attack the smaller diameter metallic SWNT. Carbon nanotubes are generally known to be radical scavengers. The met-SWNT that are covalently bonded with EAQ (density: 1.1807 g/cm^3)[36] are denser than the pristine nanotubes in DMF (density: 0.944 g/cm^3). We also observe disappearance of the metallic nanotube peaks in the UV−vis spectra of SWNT/EAQ/DMF solution when the latter is UV irradiated (at 365 nm) for 15 min without standing for a few days. In standing SWNT/DMF solution with no EAQ, no radicals are formed and no separation takes place at subsequent centrifugation of the solution.

TABLE 2: Change of Abundance of Metallic Species (using Raman and/or UV−vis−NIR) after EAQ Separation

species	diameter	chiral angle	M_{11} (eV)	ω_{RBM} (nm)	change
5,5	0.688	30	2.91	338	↓
6,6	0.825	30	2.60	283	↓
7,4	0.75	21.1	2.61	308	↓
8,5	0.89	22.4	2.43	265	same

TABLE 3: Ab Initio Calculated Binding Energies (eV) of Adsorbants with Various SWNT Species

			binding energy (eV)	
	type	diameter (Å)	EAQ	•OH
(6,4)	sc	6.92	∼0	−1.40
(6,5)	sc	7.56	∼0	−1.24
(7,4)	m	7.63	∼0	−1.52
(8,2)	m	7.27	∼0	−1.77
(7,5)	sc	8.27	∼0	−1.20
(8,4)	sc	8.29	∼0	−1.27
(10,1)	m	8.34	∼0	−1.54

To further confirm the radical involvement in the mechanism of the observed selectivity of EAQ, two similar molecules, specifically 2-ethylanthracene (EAC) and 2-(hydroxymethyl)-anthraquinone (HMAQ), were also investigated. Figure 4b) shows that HMAQ also discriminates between metallic and semiconducting CoMoCAT SWNT while EAC does not. Comparison of the structures of the three molecules (Figure 1a−c) indicates that the two molecules with metallicity-based discrimination contain carbonyl linkages which can form radicals while the other does not. The selectivity of tetrachlorobenzoquinone (TCBQ) was also investigated and was found to be poor (Supporting Information).

We also found that EAQ does not selectively deplete metallic tubes in samples of larger diameter SWNT grades, such as HiPco SWNT (0.9−1.1 nm) or Arc-discharge SWNT (1.2−1.6 nm). Possibly, the radicals do not attack the larger diameter nanotubes or the difference between small-diameter semiconducting and larger diameter metallic nanotubes in these types of samples with wide range of diameter and chiralities is small. To improve separation for other grades of SWNT, diameter selection can be conducted before applying EAQ separation. The search is ongoing in our lab for various aromatic ring structure compounds which may be more effective for larger diameter SWNT.

4. Conclusion

In summary, the present result demonstrates a simple method for enriching CoMoCAT SWNT samples in semiconducting species using the small aromatic molecule 2-ethylanthraquinone. Devices made with EAQ-separated SWNT exhibit mobilities of 0.2 cm^2/(V s) and on/off ratios of 10^4. The on/off ratios are greatly improved (∼2 orders of magnitude) over those of TFTs made with pristine SWNT. Density functional simulations using EAQ and •OH radical show that EAQ does not interact with SWNT while •OH radical preferentially attacks SWNT species in the order of small-diameter metallic, followed by small-diameter semiconducting SWNT in preference to larger diameter semiconducting SWNT. The TFT performance data, PLE maps, Raman spectra, and UV−vis−NIR spectra corroborate the finding that smaller diameter metallic SWNT are removed and larger diameter semiconducting species are enriched by treatment with EAQ in DMF. We believe that our reported simple treatment of standing CoMoCAT SWNT/EAQ/DMF in ambient

conditions will be widely applicable for obtaining semiconducting tubes for printed electronic devices.

Acknowledgment. The work was supported by a Competitive Research Program grant from the Singapore National Research Foundation (NRF-CRP2-2007-02).

Supporting Information Available: Results of separation using TCBQ (tetrachlorobenzoquinone). This material is available free of charge via the Internet at http://pubs.acs.org.

References and Notes

(1) Tans, S. J.; Verschueren, A. R. M.; Dekker, C. Room-temperature transistor based on a single carbon nanotube. *Nature* **1998**, *393* (6680), 49–52.

(2) Collins, P. C.; Arnold, M. S.; Avouris, P. Engineering carbon nanotubes and nanotube circuits using electrical breakdown. *Science* **2001**, *292* (5517), 706–709.

(3) Baughman, R. H.; Zakhidov, A. A.; de Heer, W. A. Carbon nanotubes - the route toward applications. *Science* **2002**, *297* (5582), 787–792.

(4) Snow, E. S.; Novak, J. P.; Campbell, P. M.; Park, D. Random networks of carbon nanotubes as an electronic material. *Appl. Phys. Lett.* **2003**, *82* (13), 2145–2147.

(5) Hu, L.; Hecht, D. S.; Gruner, G. Percolation in transparent and conducting carbon nanotube networks. *Nano Lett.* **2004**, *4* (12), 2513–2517.

(6) Lee, C. W.; Han, X. D.; Chen, F. M.; Wei, J.; Chen, Y.; Chan-Park, M. B.; Li, L. J. Solution-Processable Carbon Nanotubes for Semiconducting Thin-Film Transistor Devices. *Adv. Mater.* **2010**, *22* (11), 1278–1282.

(7) Cao, Q.; Kim, H. S.; Pimparkar, N.; Kulkarni, J. P.; Wang, C. J.; Shim, M.; Roy, K.; Alam, M. A.; Rogers, J. A. Medium-scale carbon nanotube thin-film integrated circuits on flexible plastic substrates. *Nature* **2008**, *454* (7203), 495–U4.

(8) Zhang, Z. Y.; Wang, S.; Ding, L.; Liang, X. L.; Pei, T.; Shen, J.; Xu, H. L.; Chen, O.; Cui, R. L.; Li, Y.; Peng, L. M. Self-Aligned Ballistic n-Type Single-Walled Carbon Nanotube Field-Effect Transistors with Adjustable Threshold Voltage. *Nano Lett.* **2008**, *8* (11), 3696–3701.

(9) Engel, M.; Small, J. P.; Steiner, M.; Freitag, M.; Green, A. A.; Hersam, M. C.; Avouris, P. Thin Film Nanotube Transistors Based on Self-Assembled, Aligned, Semiconducting Carbon Nanotube Arrays. *ACS Nano* **2008**, *2* (12), 2445–2452.

(10) Krupke, R.; Linden, S.; Rapp, M.; Hennrich, F. Thin films of metallic carbon nanotubes prepared by dielectrophoresis. *Adv. Mater.* **2006**, *18* (11), 1468–14720.

(11) Krupke, R.; Hennrich, F.; Weber, H. B.; Kappes, M. M.; von Lohneysen, H. Simultaneous deposition of metallic bundles of single-walled carbon nanotubes using ac-dielectrophoresis. *Nano Lett.* **2003**, *3* (8), 1019–1023.

(12) Krupke, R.; Hennrich, F.; von Lohneysen, H.; Kappes, M. M. Separation of metallic from semiconducting single-walled carbon nanotubes. *Science* **2003**, *301* (5631), 344–347.

(13) Hersam, M. C. Progress towards monodisperse single-walled carbon nanotubes. *Nat. Nanotechnol.* **2008**, *3* (7), 387–394.

(14) Maeda, Y.; Kimura, S.; Kanda, M.; Hirashima, Y.; Hasegawa, T.; Wakahara, T.; Lian, Y. F.; Nakahodo, T.; Tsuchiya, T.; Akasaka, T.; Lu, J.; Zhang, X. W.; Gao, Z. X.; Yu, Y. P.; Nagase, S.; Kazaoui, S.; Minami, N.; Shimizu, T.; Tokumoto, H.; Saito, R. Large-scale separation of metallic and semiconducting single-walled carbon nanotubes. *J. Am. Chem. Soc.* **2005**, *127* (29), 10287–10290.

(15) Maeda, Y.; Kanda, M.; Hashimoto, M.; Hasegawa, T.; Kimura, S.; Lian, Y. F.; Wakahara, T.; Akasaka, T.; Kazaoui, S.; Minami, N.; Okazaki, T.; Hayamizu, Y.; Hata, K.; Lu, J.; Nagase, S. Dispersion and separation of small-diameter single-walled carbon nanotubes. *J. Am. Chem. Soc.* **2006**, *128* (37), 12239–12242.

(16) Arnold, M. S.; Green, A. A.; Hulvat, J. F.; Stupp, S. I.; Hersam, M. C. Sorting carbon nanotubes by electronic structure using density differentiation. *Nat. Nanotechnol.* **2006**, *1* (1), 60–65.

(17) Tanaka, T.; Jin, H.; Miyata, Y.; Fujii, S.; Suga, H.; Naitoh, Y.; Minari, T.; Miyadera, T.; Tsukagoshi, K.; Kataura, H. Simple and Scalable Gel-Based Separation of Metallic and Semiconducting Carbon Nanotubes. *Nano Lett.* **2009**, *9* (4), 1497–1500.

(18) Li, H. P.; Zhou, B.; Lin, Y.; Gu, L. R.; Wang, W.; Fernando, K. A. S.; Kumar, S.; Allard, L. F.; Sun, Y. P. Selective interactions of porphyrins with semiconducting single-walled carbon nanotubes. *J. Am. Chem. Soc.* **2004**, *126* (4), 1014–1015.

(19) Wang, W.; Fernando, K. A. S.; Lin, Y.; Meziani, M. J.; Veca, L. M.; Cao, L.; Zhang, P.; Kimani, M. M.; Sun, Y. P. Metallic single-walled carbon nanotubes for conductive nanocomposites. *J. Am. Chem. Soc.* **2008**, *130* (4), 1415–1419.

(20) Nish, A.; Hwang, J. Y.; Doig, J.; Nicholas, R. J. Highly selective dispersion of singlewalled carbon nanotubes using aromatic polymers. *Nat. Nanotechnol.* **2007**, *2* (10), 640–646.

(21) Miyata, Y.; Maniwa, Y.; Kataura, H. Selective oxidation of semiconducting single-wall carbon nanotubes by hydrogen peroxide. *J. Phys. Chem. B* **2006**, *110* (1), 25–29.

(22) Zheng, M.; Diner, B. A. Solution Redox Chemistry of Carbon Nanotubes. *J. Am. Chem. Soc.* **2004**, *126* (47), 15490–15494.

(23) Zheng, M.; Jagota, A.; Semke, E. D.; Diner, B. A.; McLean, R. S.; Lustig, S. R.; Richardson, R. E.; Tassi, N. G. DNA-assisted dispersion and separation of carbon nanotubes. *Nat. Mater.* **2003**, *2* (5), 338–342.

(24) Chen, F. M.; Wang, B.; Chen, Y.; Li, L. J. Toward the extraction of single species of single-walled carbon nanotubes using fluorene-based polymers. *Nano Lett.* **2007**, *7* (10), 3013–3017.

(25) Kanungo, M.; Lu, H.; Malliaras, G. G.; Blanchet, G. B. Suppression of Metallic Conductivity of Single-Walled Carbon Nanotubes by Cycloaddition Reactions. *Science* **2009**, *323* (5911), 234–237.

(26) Strano, M. S.; Dyke, C. A.; Usrey, M. L.; Barone, P. W.; Allen, M. J.; Shan, H. W.; Kittrell, C.; Hauge, R. H.; Tour, J. M.; Smalley, R. E. Electronic structure control of single-walled carbon nanotube functionalization. *Science* **2003**, *301* (5639), 1519–1522.

(27) Peng, X. B.; Komatsu, N.; Kimura, T.; Osuka, A. Improved optical enrichment of SWNT through extraction with chiral nanotweezers of 2,6-pyridylene-bridged diporphyrins. *J. Am. Chem. Soc.* **2007**, *129* (51), 15947–15953.

(28) Naumov, A. V.; Kuznetsov, O. A.; Harutyunyan, A. R.; Green, A. A.; Hersam, M. C.; Resasco, D. E.; Nikolaev, P. N.; Weisman, R. B. Quantifying the Semiconducting Fraction in Single-Walled Carbon Nanotube Samples through Comparative Atomic Force and Photoluminescence Microscopies. *Nano Lett.* **2009**, *9* (9), 3203–3208.

(29) Perdew, J. P.; Burke, K.; Ernzerhof, M. Generalized gradient approximation made simple. *Phys. Rev. Lett.* **1996**, *77* (18), 3865–3868.

(30) Kresse, G.; Furthmuller, J. Efficient iterative schemes for ab initio total-energy calculations using a plane-wave basis set. *Phys. Rev. B* **1996**, *54* (16), 11169–11186.

(31) Bachilo, S. M.; Strano, M. S.; Kittrell, C.; Hauge, R. H.; Smalley, R. E.; Weisman, R. B. Structure-Assigned Optical Spectra of Single-Walled Carbon Nanotubes. *Science* **2002**, *298* (5602), 2361–2366.

(32) Jorio, A.; Santos, A. P.; Ribeiro, H. B.; Fantini, C.; Souza, M.; Vieira, J. P. M.; Furtado, C. A.; Jiang, J.; Saito, R.; Balzano, L.; Resasco, D. E.; Pimenta, M. A. Quantifying carbon-nanotube species with resonance Raman scattering. *Phys. Rev. B* **2005**, *72* (7), 075207.

(33) Maeda, Y.; Kanda, M.; Hashimoto, M.; Hasegawa, T.; Kimura, S.-i.; Lian, Y.; Wakahara, T.; Akasaka, T.; Kazaoui, S.; Minami, N.; Okazaki, T.; Hayamizu, Y.; Hata, K.; Lu, J.; Nagase, S. Dispersion and Separation of Small-Diameter Single-Walled Carbon Nanotubes. *J. Am. Chem. Soc.* **2006**, *128* (37), 12239–12242.

(34) Woods, L. M.; Badescu, S. C.; Reinecke, T. L. Adsorption of simple benzene derivatives on carbon nanotubes. *Phys. Rev. B* **2007**, *75* (15), 155415.

(35) Sangermano, M.; Crivello, J. V. *Visible and Long-Wavelength Cationic Photopolymerization, in Photoinitiated Polymerization*; American Chemical Society: Washington, DC, 2003; p 242.

(36) Yaws, C. L., *Yaws' transport properties of chemicals and hydrocarbons*; Knovel: New York, NY, 2010.

JP106398K

Supporting Information

We have also tried to use TCBQ (tetrachlorobenzoquinone) for the separation:

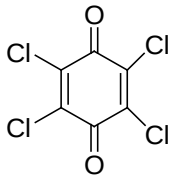

tetrachlorobenzoquinone

Under the same conditions as EAQ, after sonication in TCBQ/DMF solution the SWNTs do not disperse well in DMF solution. Almost all SWNTs precipitated in one hour so that only a very small amount of SWNTs remained in the supernatant. The supernatant was carefully collected and filtered. The solid SWNTs were washed and re-dispersed in SDS solution and the UV-vis-NIR spectrum was measured. From the UV-vis-NIR spectrum below, the M_{11} peaks in 400-490 nm are decreased but not totally suppressed.

As TCBQ is much more reactive with SWNTs than EAQ, it very easily attacks SWNTs in a short time so that the amount of SWNTs remaining in the supernatant is very small. Because of the very low yield of suspended SWNTs, TCBQ is not suitable for metallicity-based separation SWNTs. The redox potential (the electron-accepting ability) of TCBQ is (0.227 V), much higher than EAQ (-0.942 V), which means that TCBQ more readily forms radicals to attack SWNTs than does EAQ[a]. The redox potential of TCBQ is high enough to directly receive the electrons from the valence band (V1) of semiconducting species so that metallic (m) and semiconducting (S) nanotubes cannot be easily discriminated. By contrast, EAQ is weak in redox so that EAQ is only able to access the electrons from metallic tubes (as there are always electrons between V1 and C1), but not able to reach the V1 electrons of S tubes (there is no electrons in between V1 and C1 in S tubes).

We did not experimentally test benzoquinone as a separation agent. However, the redox potential of benzoquinone is -0.255 V so that, like TCBQ, it may be too reactive and non-discriminatory between metallic and semiconducting [a].

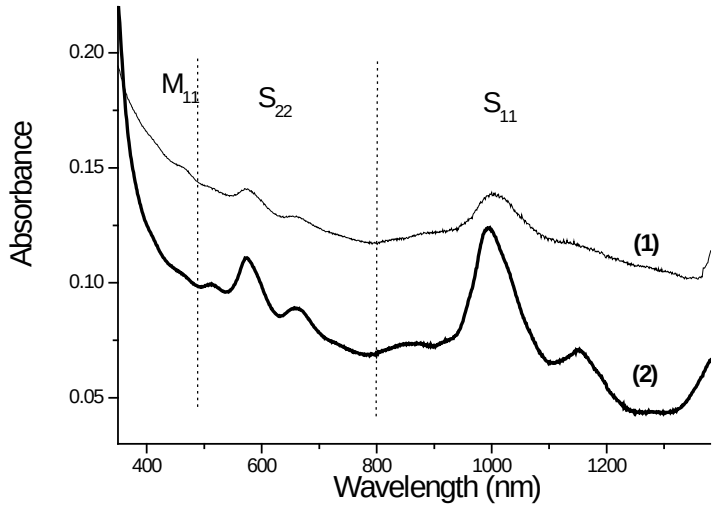

Fig S1. Optical absorption spectra of (1) SWNTs after treatment with TCBQ (2) SWNTs after treatment with EAQ

Reference

a Zhu X.Q.; Chun H.W. Accurate Estimation of the One-Electron Reduction Potentials of Various Substituted Quinones in DMSO and CH_3CN *J. Org. Chem.* **2010**, *75*, 5037–5047